This manuscript has been published in Spectrochimica Acta Part A: Molecular and Biomolecular Spectroscopy 261 (2021) 120005 doi: https://doi.org/10.1016/j.saa.2021.120005

Hyperspectral z-scan: Measurement of spectrally resolved nonlinear optical properties

Maria Merin Antony,[a] C. S. Suchand Sandeep,[a,*] and Vadakke Matham Murukeshan [a,*]

[a] *Centre for Optical and Laser Engineering, School of Mechanical and Aerospace Engineering, Nanyang Technological University, 50 Nanyang Avenue, 639798, Singapore.*

Abstract

Broadband hyperspectral z-scan using a supercontinuum light source is a convenient technique to obtain spectrally resolved nonlinear optical properties of the materials under investigation. Post-processing and segregation of the data obtained from the supercontinuum based hyperspectral z-scan measurement aids in determining the nonlinear optical properties with high spectral resolution. However, few data models exist to store and represent the large amount of information acquired from the hyperspectral z-scan measurement. In this paper, a 3D data model for representing the data obtained from broadband z-scan measurements and analysis is presented. This method would help in the quick characterization of spectrally resolved nonlinear optical properties of materials from a single z-scan measurement. The proposed model is used for obtaining the spectrally resolved nonlinear optical properties of rhodamine 6G.

Keywords: Nonlinear absorption, Nonlinear refraction, Z-scan, Supercontinuum, Hyperspectral, NLO

* Corresponding authors.
Email addresses: ssuchand@ntu.edu.sg (C. S. Suchand Sandeep) and mmurukeshan@ntu.edu.sg (V. M. Murukeshan)

This manuscript has been published in Spectrochimica Acta Part A: Molecular and Biomolecular Spectroscopy 261 (2021) 120005 doi: https://doi.org/10.1016/j.saa.2021.120005

1. Introduction

Measurement and analysis of spectrally resolved nonlinear optical properties are extremely important in the quest for materials exhibiting high nonlinearities for photonic applications. Techniques used for the determination of spectrally resolved features are generally classified based on the number of spectral bands or spectral resolution as multispectral, hyperspectral, and ultraspectral [1]. The number of spectral bands dealt in multispectral is around 3 to 10, while hyperspectral refers to hundreds of spectral bands. For the technique to be called ultraspectral, the number of spectral bands should be of the order of thousands [2]. These are classifications pertaining in the spectral imaging technology where the captured spectrally resolved images are processed to form data cubes. A data cube in spectral imaging is a three-dimensional (3D) representation of data where the first two dimensions are spatial (x and y axes) while the third dimension (z axis) is spectral (wavelength) [3]. Such data cubes provide a wealth of information about the sample material, which is extremely useful for its characterization.

For the determination of nonlinear optical properties, one of the most commonly used method is the z-scan technique, developed by M. Sheik-Bahae and co-workers [4]. Several interesting studies of the nonlinear optical properties of various materials such as perovskite thin films [5], dye-polymer systems [6], nanocrystals [7], nanocomposite films [8], nanowires [9], nanobelts [10], chalcogenides [11, 12] etc. were reported using the z-scan technique. Recently, graphene was studied for their nonlinear optical properties along different wavelengths [13, 14], which revealed their potential to be used in nonlinear optical signal processing [15, 16]. In another recent study, thickness-dependent nonlinear optical properties of perovskite nanosheets were investigated [17]. However, in all these reported works, the measurements were carried out using monochromatic sources. The measurement of spectrally resolved nonlinear optical properties in this scheme therefore requires an optical parametric amplifier capable of producing different wavelengths for excitation, and discrete z-scan measurements are to be carried out at each of these wavelengths, which is tedious and time-consuming. To overcome this limitation, a method known as the white-light continuum

z-scan technique was developed by M. Balu and co-workers [18]. This method allows rapid broadband nonlinear optical characterization by replacing the monochromatic sources and conventional detectors used in the traditional z-scan setup with supercontinuum sources and spectrometers respectively [18]. Recently, N. Munera and co-workers generated supercontinuum in 800 nm – 1600 nm range and demonstrated its usefulness for z-scan nonlinear spectroscopy [19]. The supercontinuum based z-scan technique can provide useful information about various nonlinear processes occurring in the sample for all the wavelengths present in the incident radiation from a single z-scan measurement. However, no data model currently exists to represent and store this big data, the massive amount of information obtained from the supercontinuum based z-scan measurements.

In this paper, we propose and demonstrate a data model for storing and analysing the broadband z-scan data. This model can represent the huge amount of spectrally resolved data in the form of a 3D surface plot, clearly presenting the spectrally resolved nonlinear characteristics of the sample. Based on the number of spectral bands resolved, the broadband z-scan measurement presented in this work is termed as hyperspectral z-scan measurement [1]. The data model is validated by performing hyperspectral z-scan measurements on a standard laser dye, rhodamine 6G, and both nonlinear refraction and nonlinear absorption spectra are evaluated and compared with values obtained from conventional z-scan measurement [20-22].

2. Experimental

The experimental system used for recording the hyperspectral z-scan data is shown in Fig. 1. A supercontinuum laser source (NKT Photonics SuperK EXTREME, 5 ps, 20 MHz) was used for exciting the sample and a fiber optic coupled spectrometer (USB4000, Ocean Optics) was used for recording the spectrally resolved nonlinear transmission. A solution of 3 mM rhodamine 6G (Product# 252433, Sigma-Aldrich) in water was taken in a cuvette of 1 mm thickness. This sample was mounted on a motorized translation stage having a step resolution of 1.25 μm. The output from the supercontinuum laser was passed

through a short pass filter of 900 nm cut-off wavelength (FES0900, Thorlabs) to remove the infra-red wavelengths present in the supercontinuum. The emission from the supercontinuum laser after the short pass filter spans over a wavelength range of 550 nm – 830 nm (see supplementary information). The data analysis in this work is limited to 600 nm - 700 nm wavelength range that had reasonable intensities to induce nonlinearity in the sample. An achromatic doublet lens of 89 mm focal length was used for focussing the incident beam on to the sample. The sample was moved along the propagation direction of the beam, symmetrically on either side of the focal point in steps of 250 μm. The transmission spectrum was recorded at each *z* position using the fiber optic spectrometer, which had a spectral resolution of 1 nm. An integrating sphere coupled to the optical fiber probe was used to collect the transmitted light from the sample. The integrating sphere helps in collecting the transmission profiles for the whole wavelength range and helps in reducing unintentional effects due to nonlinear scattering from the sample. The spectrometer was electronically triggered at each *z* position and the data was acquired using a PC. Both closed aperture and open aperture z-scan measurements were carried out on the sample to determine the nonlinear refraction and the nonlinear absorption, respectively. The experimental system was fully automated using a custom written software code to control the translational stage, trigger the spectrometer, and acquire the data.

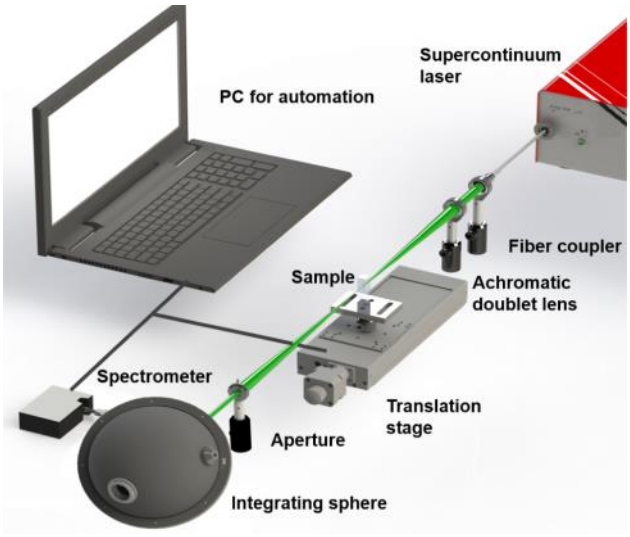

Fig. 1. Schematic of the experimental configuration of the closed aperture hyperspectral z-scan measurement.

When the sample is translated along the focused beam, the sample encounters different intensities at different *z* positions. The value of the intensity at each *z* position can be precisely calculated based on the focusing geometry. Hence the position dependent transmission data recorded in the z-scan experiment can be easily transformed to the intensity dependent transmission of the sample. In the closed aperture z-scan configuration, an aperture of 3 mm diameter was placed in front of the integrating sphere so that the beam size variation due to nonlinear refraction of the sample results in an intensity variation at the detector. The size of the aperture is carefully chosen such that it satisfied the well-established condition, $0.1 < S < 0.5$, where S is the aperture linear transmittance given by $S = 1 - \exp(-2r_a^2/\omega_a^2)$ (r_a is the aperture radius and ω_a is the beam radius at the aperture) [23]. During the open aperture z-scan measurements, the aperture was removed from the setup shown in Fig. 1 and the entire transmitted light was collected by the integrating sphere. The focal length of the focusing lens (89 mm) was chosen such that the Rayleigh length of the focused beam fulfilled the thin sample approximation criterion [4]. The Rayleigh length of the current configuration is 2.1 mm, which is larger than the sample thickness of 1 mm, fulfilling the thin sample approximation.

3. Results and Discussion

The spectra recorded from the z-scan measurements were processed using a custom written MATLAB® code for creating the hyperspectral z-scan data model. First, the recorded spectra were normalized using the linear transmission spectrum of the sample. Then the spectra recorded at different *z* positions were processed and rearranged to a *z* position versus transmission data for each specific wavelength in the spectrum. These datasets were stored in the form of matrices that were mapped to corresponding wavelengths to form a grid of matrices. This grid of matrices was used to generate the final graphic model using MATLAB®. The proposed data model can graphically represent the z-scan data along

hundreds of spectrally resolved bands in the form of a 3D surface plot called the hyperspectral z-scan data model. The process flow for generating the graphical model is presented in Fig. 2.

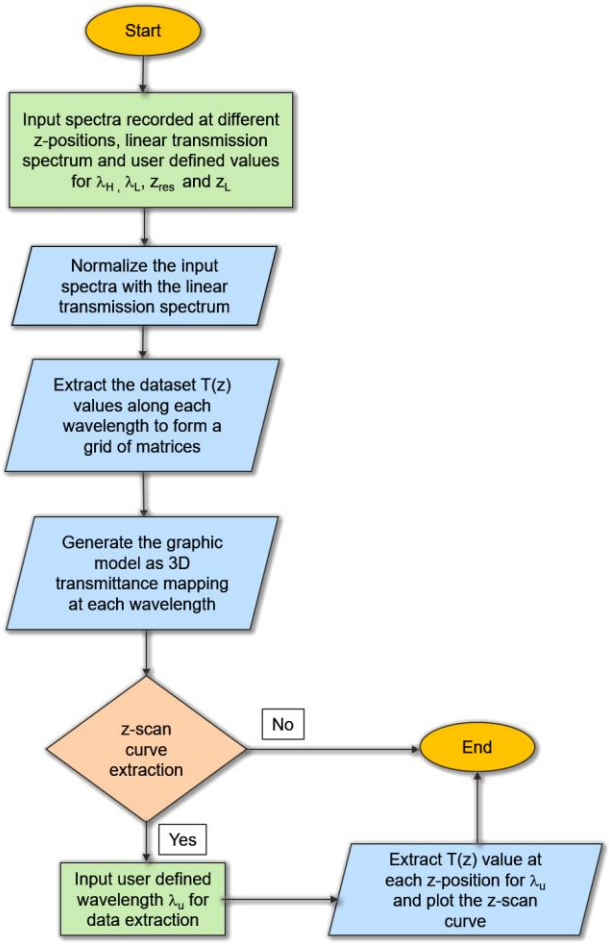

Fig. 2. Flowchart of the algorithm used for the generation of the graphical model. λ_H = upper wavelength limit, λ_L = lower wavelength limit, λ_u = user selected wavelength, z_{res} = z-scan step size, z_L = z-scan traversing length, T(z) = normalized transmittance.

The spectrally resolved z-scan data obtained from the hyperspectral closed-aperture z-scan measurement is presented in Fig. 3. For a sample exhibiting nonlinear refraction, self-focussing or self-defocussing of the beam occurs and the beam size reaching the aperture will change, resulting in an intensity variation at the detector. This intensity variation will manifest either as a peak followed by a valley (negative nonlinearity), or as a valley followed by a peak (positive nonlinearity) behaviour in the z-scan curve. From the z-scan data model presented in Fig. 3, for all the wavelengths in the measurement range of 600 nm to

700 nm, the sample exhibits nonlinear refraction. The nonlinear refraction in a material can be expressed as [24],

$$n = n_0 + n_2 I \tag{1}$$

where n_0 is the linear refractive index, I is the intensity and n_2 is the nonlinear refractive index. The nonlinear refraction curves for any wavelength in the measurement range can be extracted from the dataset and can be numerically fitted to determine the nonlinear refractive index, n_2. Eq. (2) represents the on-axis normalized transmittance for small phase shifts by adopting Gaussian decomposition method [11, 25],

$$T(z) = 1 + \frac{4x\Delta\varphi}{(1+x^2)(9+x^2)} \tag{2}$$

where x is z/z_R, z_R is the Rayleigh length and $\Delta\varphi$ is the nonlinear phase shift ($|\Delta\varphi| < \pi$). The data is numerically fitted using Eq. (2) and the value of n_2 at 650 nm is found to be -2.1×10^{-14} m^2/W. It should be noted that the nonlinear refraction observed in the sample in the present case would mainly be of thermal origin as the sample possesses non-vanishing absorption at the excitation wavelength regime. Additionally, the high repetition rate of the excitation source would result in accumulative heating of the sample and plays a crucial role in the nonlinear refraction observed [26, 27]. This is also evident from the thermal lensing type behaviour observed in the nonlinear refraction curves that show a peak followed by a valley in the transmission data.

This manuscript has been published in Spectrochimica Acta Part A: Molecular and Biomolecular Spectroscopy 261 (2021) 120005 doi: https://doi.org/10.1016/j.saa.2021.120005

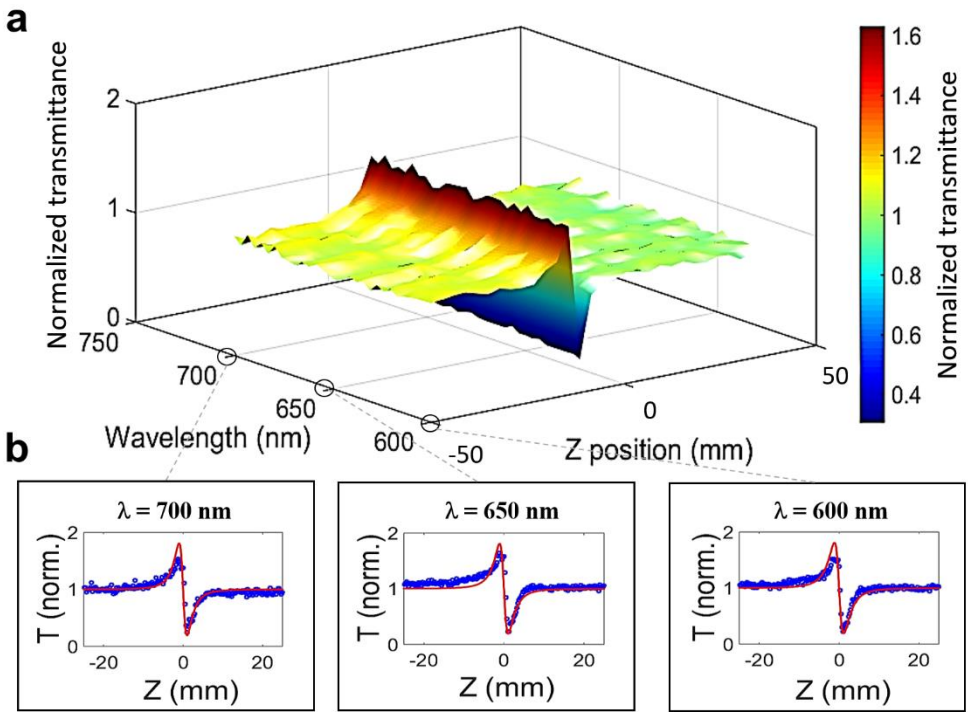

Fig. 3. (a) Hyperspectral z-scan data model representation of the closed aperture z-scan data. **(b)** Representative z-scan curves extracted from the data model at 600 nm, 650 nm, and 700 nm. The blue circles represent experimental data while the red curves represent the theoretical fit to the data.

In order to confirm the thermal origin of the nonlinearity, the closed aperture z-scan curve extracted at 650 nm from the hyperspectral z-scan data was numerically fitted using the aberrant thermal lens model. The normalized transmittance at steady state is given by [28, 29],

$$T(z) = 1 + \frac{\Delta\vartheta}{p(1+x^2)^{p-1}} \tan^{-1}\left(\frac{2px}{2p+1+x^2}\right) \quad \text{- (3)}$$

where x is z/z_R, z_R is the Rayleigh length and $\Delta\vartheta$ is the on-axis phase shift/thermal lens strength and p is the order of nonlinearity, which is taken as 2 in this case. At steady state, the phase shift $\Delta\vartheta$ is given by [30],

$$\Delta\vartheta = \frac{PL\alpha}{\lambda\kappa} \times \frac{dn}{dT} \quad \text{- (4)}$$

where P is the laser power, α is the linear absorption coefficient, L is the length of the sample, λ is the wavelength and κ is the thermal conductivity. The corresponding nonlinear refractive index can be deduced by [31],

$$n_2 = \frac{\varepsilon_0 n_0 c\alpha}{4\kappa} \times \frac{dn}{dT} \times \omega_0^2 \qquad -(5)$$

where ω_0 is the spot size. The data is numerically fitted for the thermal lens model using Eq. (3) and is shown in Fig.4. The value of n_2 is found to be -2.5 × 10^{-14} m^2/W (using Eq. (5)), which matches well with the n_2 value obtained using Sheik-Bahae formalism. The values of the n_2 obtained from the two models are given in Table 1.

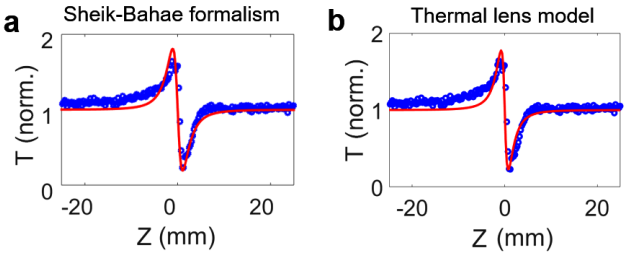

Fig. 4.Closed aperture z-scan data fitted using (a) Sheik-Bahae formalism and (b) thermal lens model. The blue circles represent experimental data and the red curves represent theoretical fit to the data.

Table 1: Nonlinear refractive index values obtained using two models

Fitting model	n_2 (m^2/W)
Thermal lens	- 2.5 × 10^{-14}
Sheik-Bahae	- 2.1 × 10^{-14}

The z-scan dataset obtained from the open aperture z-scan measurements is presented in Fig. 5. The sample shows a reduction in transmission for higher excitation intensity close to the focal point (z = 0), which is referred to as the optical limiting behaviour. The spectrally resolved z-scan curves extracted from the open aperture z-scan dataset are numerically fitted to Eq. (6), which is obtained by integrating the spatial and temporal Gaussian pulses to get the normalized transmittance equation [32],

$$T(z) = \frac{1}{\sqrt{\pi} q} \int_{-\infty}^{\infty} \ln\left(1 + q e^{-j^2}\right) dj \qquad (6)$$

where $q = \beta I_0 L_{eff}/(1+z^2/z_R^2)$, L_{eff} is the effective sample length given by $L_{eff} = (1-e^{-\alpha L})/\alpha$, L is the length of the sample, α is the linear absorption coefficient, β is the nonlinear absorption coefficient and z_R is the Rayleigh length. The two photon absorption (2PA) coefficients obtained by numerically fitting the data using Eq. (6) are of the order of 10^{-9} m/W.

This manuscript has been published in Spectrochimica Acta Part A: Molecular and Biomolecular Spectroscopy 261 (2021) 120005 doi: https://doi.org/10.1016/j.saa.2021.120005

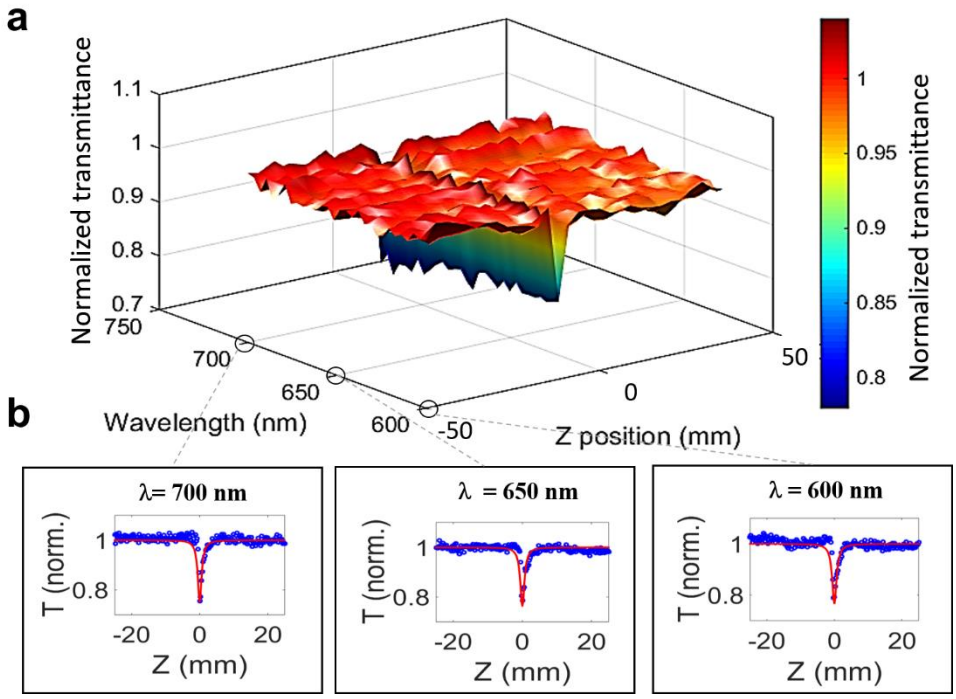

Fig. 5. (a) Hyperspectral z-scan data model representation of open aperture z-scan data. **(b)** z-scan curves extracted from the data model at 600 nm, 650 nm and 700 nm. The blue circles represent experimental data while the red curves represent theoretical fit to the data.

Fig. 6 shows the spectrally resolved 2PA coefficients plotted against the wavelength. Previous works on the two photon absorption measurements on rhodamine 6G have reported that the nonlinear absorption would have contributions from excited state absorption (ESA) and 2PA [33, 34]. The 2PA processes observed in the present scenario (shown in Fig. 5) would be the result of cumulative effects from ESA and 2PA and hence should be inferred only as an effective 2PA rather than pure electronic 2PA. Further, the relatively high concentration of rhodamine 6G used for this investigation results in dimer formation in the sample, which is evident from the absorption spectra shown in the inset of Fig. 6. The presence of the absorption peak centred at 500 nm in the linear absorption spectrum is indicative of H-dimer formation due to the aggregation of rhodamine 6G molecules [35]. It has been reported that such aggregation leads to the localization of energy in the excited states, which enhances the excited state absorption [36]. The spectrally resolved nonlinear optical properties of rhodamine 6G obtained from the hyperspectral z-scan are tabulated in Table 2. It should be noted that the nonlinear refraction in this case is caused by accumulative thermal lensing phenomenon, and hence its wavelength dependence could not be observed in this measurement.

This manuscript has been published in Spectrochimica Acta Part A: Molecular and Biomolecular Spectroscopy 261 (2021) 120005 doi: https://doi.org/10.1016/j.saa.2021.120005

The thermal origin of the nonlinear refraction is further verified by reducing the repetition rate of the pump beam with the help of an optical chopper. The nonlinear refraction completely vanishes upon reducing the repetition rate of the pump beam with the help of an optical chopper running at 2 kHz. However, the nonlinear absorption remains the same even under the reduced repetition rate and its magnitude is not affected by the thermal nonlinearity (see Fig. S2).

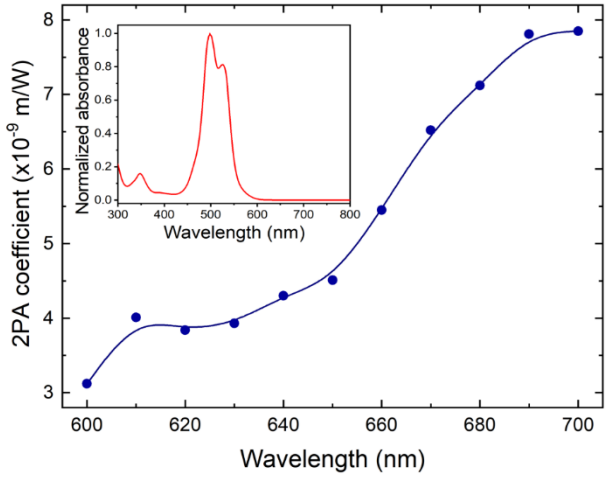

Fig. 6. Plot of 2PA coefficients computed from the hyperspectral z-scan data in 10 nm intervals from 600 nm to 700 nm. The line is only a guide to the eye. Inset shows the linear absorption spectrum of 3 mM rhodamine 6G.

Table 2: Spectrally resolved nonlinear optical properties of rhodamine 6G obtained from the hyperspectral z-scan measurement.

Wavelength, λ (nm)	Spot size, ω_0 (µm)	Beam Intensity, I_0 ($\times 10^{11}$ W/m^2)	Effective 2PA coefficient, β_{eff} ($\times 10^{-9}$ m/W)	Nonlinear refractive index, n_2 ($\times 10^{-14}$ m^2/W)
600	17.3	1.20	3.1	-2.1
610	17.6	1.40	4.0	-2.1
620	17.9	1.11	3.8	-2.0
630	18.2	0.90	3.9	-2.1
640	18.5	0.81	4.2	-2.0
650	18.8	0.75	4.5	-2.1
660	19.1	0.80	5.5	-2.1
670	19.3	0.74	6.5	-2.1
680	19.6	0.72	7.1	-2.0
690	19.9	0.70	7.8	-2.0
700	20.2	0.61	7.9	-2.2

For validating the values of the nonlinear refractive index and effective 2PA coefficients obtained using the hyperspectral z-scan, conventional z-scan measurements under similar experimental conditions were carried out on the sample. For conducting the conventional z-scan measurements, monochromatic excitation was achieved by the use of a narrowband filter of 650 nm (10 nm FWHM) in the same supercontinuum laser beam. This method was chosen over using a completely different laser source in order to keep the experimental parameters as close to the hyperspectral z-scan experimental conditions as possible. The results obtained from the conventional z-scan measurements are compared to the results obtained from the hyperspectral z-scan measurement, and are shown in Fig. 7. The nonlinear optical coefficients obtained from the two measurements are presented in Table 3. It can be seen that the values obtained from hyperspectral z-scan and conventional z-scan matches quite well with each other. The slightly higher values obtained for the nonlinear refraction in the hyperspectral z-scan measurement can be attributed to the non-degenerate thermal lensing effect arising from the broadband excitation.

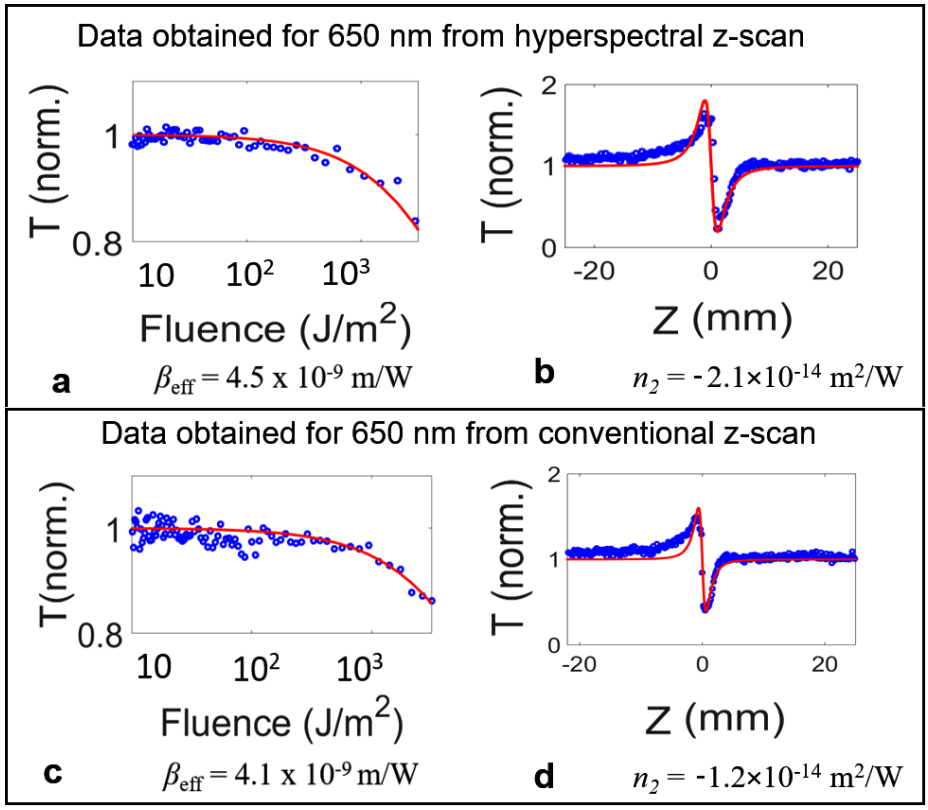

Fig. 7. Fluence and z-scan curves at 650 nm. (a) Open aperture fluence data obtained using hyperspectral z-scan measurement. (b) Closed aperture z-scan data obtained using hyperspectral z-scan measurement. (c) Open aperture fluence data obtained from conventional z-scan measurement. (d) Closed aperture z-scan data obtained from conventional z-scan measurement. The blue circles represent experimental data and the red curves represent theoretical fit to the data.

Table 3: Nonlinear optical coefficients obtained using hyperspectral z-scan and conventional z-scan

Type of measurement	β_{eff} (m/W)	n_2 (m^2/W)
Hyperspectral z-scan	4.5×10^{-9}	$- 2.1 \times 10^{-14}$
Conventional z-scan	4.1×10^{-9}	$- 1.2 \times 10^{-14}$

Though there are several reports on the nonlinear optical properties of materials at a single wavelength, only a few reports present spectrally resolved nonlinear optical coefficients of the materials under investigation. This is mainly owing to the tedious amount of measurements required when using the conventional z-scan technique. The supercontinuum based hyperspectral z-scan technique presented in this paper shows an elegant way of extracting spectrally resolved nonlinear optical coefficients from a single z-scan measurement and representing them in an easy to comprehend fashion. We envisage this to become the potential model for the representation of spectrally resolved z-scan data in future works.

4. Conclusion

We have proposed and illustrated a new data model for representing the spectrally resolved data obtained from hyperspectral z-scan measurements. The data model developed provides an abstract representation of the nonlinear absorption and nonlinear refraction behavior of the sample. The 3D model not only presents a pictorial representation of z-scan curves arranged along well-defined spectral points, but also provides a method to extract the various nonlinear optical coefficients from the data. The proposed model is demonstrated by representing the data obtained from a supercontinuum based z-scan experiment on a standard laser dye, rhodamine 6G, and the spectrally resolved nonlinear optical coefficients are analysed using the data model. The results correlate well with results obtained using conventional z-scan measurements, validating the proposed model. Future works in this research will be aimed at the study of the nondegenerate effects on the nonlinear optical coefficients. The proposed method helps in the quick

determination of spectrally resolved two-photon absorption coefficients and nonlinear refractive indices of materials.

CRediT authorship contribution statement

Maria Merin Antony: Methodology, Investigation, Software, Visualization, Formal analysis, Data curation, Writing - original draft. C.S. Suchand Sandeep: Conceptualization, Methodology, Investigation, Software, Formal analysis, Visualization, Writing - review & editing. Vadakke Matham Murukeshan: Conceptualization, Supervision, Funding acquisition, Writing - review & editing.

Declaration of competing interest

The authors declare that they have no known competing financial interests or personal relationships that could have appeared to influence the work reported in this paper.

Acknowledgement

The authors acknowledge NTU-India Connect programme and COLE-EDB, NTU for funding and research manpower support.

Appendix A. Supplementary material

See supplementary material for the emission spectrum of the supercontinuum laser used for the measurements and the comparison of the results obtained from high-repetition rate and lower repetition rate hyperspectral z-scan measurements.

References

[1] S.K. Park, J.J. Puschell, Z.-u. Rahman, Hyperspectral imagers for current and future missions, Visual Information Processing IX, (2000) 121-132. doi: http://doi.org/10.1117/12.390476

[2] V. Fresse, D. Houzet, C. Gravier, GPU architecture evaluation for multispectral and hyperspectral image analysis, 2010 Conference on Design and Architectures for Signal and Image Processing (DASIP), (2010) 121-127. doi: http://doi.org/10.1109/dasip.2010.5706255

[3] H.T. Lim, V.M. Murukeshan, A four-dimensional snapshot hyperspectral video-endoscope for bio-imaging applications, Scientific Reports, 6 (2016) 24044. doi: http://doi.org/10.1038/srep24044

[4] M. Sheik-Bahae, A.A. Said, E.W. Van Stryland, High-sensitivity, single-beam n(2) measurements, Optics Letters, 14 (1989) 955-957. doi: http://doi.org/10.1364/ol.14.000955

[5] R.A. Ganeev, K.S. Rao, Z. Yu, et al., Strong nonlinear absorption in perovskite films, Optical Materials Express, 8 (2018) 1472. doi: http://doi.org/10.1364/ome.8.001472

[6] G. Sreekumar, P.G. Louie Frobel, S. Sreeja, et al., Nonlinear absorption and photoluminescence emission in nanocomposite films of Fuchsine Basic dye–polymer system, Chemical Physics Letters, 506 (2011) 61-65. doi: http://doi.org/10.1016/j.cplett.2011.02.048

[7] A.A. Said, M. Sheik-Bahae, D.J. Hagan, et al., Determination of bound-electronic and free-carrier nonlinearities in ZnSe, GaAs, CdTe, and ZnTe, Journal of the Optical Society of America B, 9 (1992) 405. doi: http://doi.org/10.1364/josab.9.000405

[8] B. Karthikeyan, M. Anija, P. Venkatesan, et al., Ultrafast optical power limiting in free-standing Pt–polyvinyl alcohol nanocomposite films synthesized in situ, Optics Communications, 280 (2007) 482-486. doi: http://doi.org/10.1016/j.optcom.2007.08.046

[9] K. Wang, J. Zhou, L. Yuan, et al., Anisotropic third-order optical nonlinearity of a single ZnO micro/nanowire, Nano Letters, 12 (2012) 833-838. doi: http://doi.org/10.1021/nl203884j

[10] M.R. Parida, C. Vijayan, C.S. Rout, et al., Enhanced optical nonlinearity in β-AgVO3 nanobelts on decoration with Ag nanoparticles, Applied Physics Letters, 100 (2012) 121119. doi: http://doi.org/10.1063/1.3696301

[11] X. Zheng, Y. Zhang, R. Chen, et al., Z-scan measurement of the nonlinear refractive index of monolayer WS(2), Optics Express, 23 (2015) 15616-15623. doi: http://doi.org/10.1364/OE.23.015616

[12] A.R. Barik, K.V. Adarsh, R. Naik, et al., Photoinduced transparency of effective three-photon absorption coefficient for femtosecond laser pulses in Ge16As29Se55 thin films, Applied Physics Letters, 98 (2011) 201111. doi: http://doi.org/10.1063/1.3591978

[13] K.J. Ahn, J.Y. Gwak, B.J. Lee, et al., Wavelength and fluence-dependent third-order optical nonlinearity of mono- and multi-layer graphene, Applied Optics, 56 (2017) 9920. doi: http://doi.org/10.1364/ao.56.009920

[14] H. Zhang, S. Virally, Q. Bao, et al., Z-scan measurement of the nonlinear refractive index of graphene, Optics Letters, 37 (2012) 1856-1858. doi: http://doi.org/10.1364/OL.37.001856

[15] J. Wang, X. Hu, Recent Advances in Graphene-Assisted Nonlinear Optical Signal Processing, Journal of Nanotechnology, 2016 (2016) 1-18. doi: http://doi.org/10.1155/2016/7031913

[16] J.W. You, S.R. Bongu, Q. Bao, et al., Nonlinear optical properties and applications of 2D materials: theoretical and experimental aspects, Nanophotonics, 8 (2018) 63-97. doi: http://doi.org/10.1515/nanoph-2018-0106

[17] J. Zhang, T. Jiang, X. Zheng, et al., Thickness-dependent nonlinear optical properties of CsPbBr3 perovskite nanosheets, Optics Letters, 42 (2017) 3371-3374. doi: http://doi.org/10.1364/OL.42.003371

[18] M. Balu, J. Hales, D. Hagan, et al., White-light continuum Z-scan technique for nonlinear materials characterization, Optics Express, 12 (2004) 3820-3826. doi: http://doi.org/10.1364/opex.12.003820

[19] N. Munera, P. Zhao, R.A. Herrera, et al., Broadband Near Infrared Supercontinuum for Z-Scan Nonlinear Spectrometer, Frontiers in Optics 2017, OSA Technical Digest (online) (Optical Society of America, 2017), paper JW3A.9., (2017). doi: http://doi.org/10.1364/FIO.2017.JW3A.9

[20] D. Yan, S. You-Yi, W. Pei, et al., Effect of Ag Nanoparticles on Optical Properties of R6G Doped PMMA Films, Chinese Physics Letters, 24 (2007) 954-956. doi: http://doi.org/10.1088/0256-307x/24/4/029

[21] P. Sperber, A. Penzkofer, S0-S n two-photon absorption dynamics of rhodamine dyes, Optical and Quantum Electronics, 18 (1986) 381-401. doi: http://doi.org/10.1007/bf02032565

[22] J.P. Hermann, J. Ducuing, Dispersion of the two-photon cross section in rhodamine dyes, Optics Communications, 6 (1972) 101-105. doi: http://doi.org/10.1016/0030-4018(72)90204-0

[23] M.G. Kuzyk, C.W. Dirk, Characterization Techniques and Tabulations for Organic Nonlinear Materials, Marcel Dekker, New York, 1998.

[24] R.W. Boyd, Nonlinear Optics, Academic Press, London, 2003.

[25] M. Sheik-Bahae, A.A. Said, T.H. Wei, et al., Sensitive measurement of optical nonlinearities using a single beam, IEEE Journal of Quantum Electronics, 26 (1990) 760-769. doi: http://doi.org/10.1109/3.53394

[26] A. Gnoli, L. Razzari, M. Righini, Z-scan measurements using high repetition rate lasers: how to manage thermal effects, Optics Express, 13 (2005) 7976-7981. doi: http://doi.org/10.1364/opex.13.007976

[27] A. Shehata, T. Mohamed, Method for an accurate measurement of nonlinear refractive index in the case of high-repetition-rate femtosecond laser pulses, Journal of the Optical Society of America B, 36 (2019) 1246. doi: http://doi.org/10.1364/josab.36.001246

[28] Sakshi, B.C. Swain, A.K. Das, et al., Probing third-order nonlinearity in serotonin: A Z-scan study, Spectrochimica Acta Part A: Molecular and Biomolecular Spectroscopy, 223 (2019) 117319. doi: http://doi.org/10.1016/j.saa.2019.117319

[29] M. Falconieri, Thermo-optical effects in Z -scan measurements using high-repetition-rate lasers, Journal of Optics A: Pure and Applied Optics, 1 (1999) 662-667. doi: http://doi.org/10.1088/1464-4258/1/6/302

[30] U. Tripathy, P.B. Bisht, Influence of pulsed and cw pumping on optical nonlinear parameters of laser dyes probed by a closed-aperture Z-scan technique, Journal of the Optical Society of America B, 24 (2007) 2147. doi: http://doi.org/10.1364/josab.24.002147

[31] F.L.S.A. Cuppo, A.M. Figueiredo Neto, S.L. Gómez, et al., Thermal-lens model compared with the Sheik-Bahae formalism in interpreting Z-scan experiments on lyotropic liquid crystals, Journal of the Optical Society of America B, 19 (2002) 1342. doi: http://doi.org/10.1364/josab.19.001342

[32] J. Wang, B. Gu, H.-T. Wang, et al., Z-scan analytical theory for material with saturable absorption and two-photon absorption, Optics Communications, 283 (2010) 3525-3528. doi: http://doi.org/10.1016/j.optcom.2010.05.007

[33] C. Rullière, P. Kottis, Two-photon spectroscopy of organic molecules recorded by the fluorescence induced by a picosecond light continuum generated in D2O, Chemical Physics Letters, 75 (1980) 478-482. doi: http://doi.org/10.1016/0009-2614(80)80559-8

[34] P. Sathy, R. Philip, V.P.N. Nampoori, et al., Photoacoustic observation of excited singlet state absorption in the laser dye rhodamine 6G, Journal of Physics D: Applied Physics, 27 (1994) 2019-2022. doi: http://doi.org/10.1088/0022-3727/27/10/005

[35] M. Chapman, W.B. Euler, Rhodamine 6G Structural Changes in Water/Ethanol Mixed Solvent, Journal of Fluorescence, 28 (2018) 1431-1437. doi: http://doi.org/10.1007/s10895-018-2318-0

[36] S. Venugopal Rao, N.K.M. Naga Srinivas, D. Narayana Rao, Nonlinear absorption and excited state dynamics in Rhodamine B studied using Z-scan and degenerate four wave mixing techniques, Chemical Physics Letters, 361 (2002) 439-445. doi: http://doi.org/10.1016/s0009-2614(02)00928-4